Calculations of the Stratospheric Quasi-Biennial Oscillation for Time-Varying Wave Forcing

MARVIN A. GELLER, WEIXING SHEN, MINGHUA ZHANG, AND WEI-WU TAN

Institute for Terrestrial and Planetary Atmospheres, State University of New York at Stony Brook, Stony Brook, New York

(Manuscript received 31 August 1995, in final form 20 September 1996)

ABSTRACT

One-dimensional calculations are carried out for the time evolution of the equatorial lower stratospheric mean zonal wind forced by time-varying equatorial Kelvin and mixed Rossby–gravity waves. If the time variation of the wave momentum forcing is given by a steady forcing plus a sinusoidal modulation, a tendency toward phase locking between the period of the wave forcing's modulation and the period of the resulting mean wind oscillation is found in some cases, depending on the period and magnitude of the wave forcing as well as the phase difference between variations of the easterly and westerly momentum fluxes. Regime diagrams are shown to make these dependences clearer. If the wave forcings are irregularly modulated, the resulting time variation of the wind oscillation shows no resemblance to the imposed time variation of the wave forcing. These simple calculations are used to indicate that for nonlinear phenomena, such as the quasi-biennial oscillation (QBO), one cannot conclude that a lack of correlation between two data records means that these are physically unrelated. When the equatorial wave momentum fluxes are modulated according to the eastern Pacific sea surface temperatures, the simulated time variation of the QBO period sometimes (depending on the phase relation between the easterly and westerly time-varying fluxes) shows a great resemblance to the observations. This suggests that easterly and westerly momentum fluxes into the equatorial lower stratosphere are related to SST variations.

1. Introduction

The quasi-biennial oscillation (QBO) in the lower stratospheric equatorial mean zonal winds was discovered independently by Reed et al. (1961) and Veryard and Ebdon (1961). About one decade after the QBO's discovery, Lindzen and Holton (1968) and Holton and Lindzen (1972), hereafter referred to as LH and HL, respectively, proposed their theory in which the QBO is forced by eastward and westward propagating equatorial waves originating in the troposphere; LH and HL suggested that the waves responsible for forcing the QBO were the equatorial Kelvin and mixed Rossby–gravity waves. Research on this topic has progressed since the papers of LH and HL to include two- and three-dimensional models of the QBO (e.g., Plumb and Bell 1982; Takahashi and Boville 1992) and to include forcing by a spectrum of waves (Saravanan 1990). Both observational analysis (Lindzen and Tsay 1975) and three-dimensional modeling (Takahashi and Boville 1992) indicate that the easterly and westerly momentum sources from equatorial mixed Rossby–gravity waves and Kelvin waves do not appear to be sufficient to force the observed QBO. Suggestions have been made that equatorial gravity waves may play a crucial role in providing the needed momentum sources.

One aspect of the QBO that has not been explored a great deal is the role that time-varying sources of equatorial waves might have in forcing the QBO. There is certainly an expectation that the wave momentum fluxes forcing the QBO will vary with time. Although there are several theories as to the source of these waves, many of them predict that there should be a variation in these wave fluxes in response to sea surface temperature (SST) variations. Thus, since the sea surface temperatures vary from year to year, it is reasonable to suppose that the equatorial waves might also vary in a related manner, so we inquire how interannual variations in equatorial waves might affect the QBO. There have been several investigations suggesting relations between the stratospheric QBO and QBO variations in the troposphere and SSTs (e.g., Yasunari 1989), while others have suggested that there is no evidence of any coherence between the lower stratospheric QBO and SST variations (e.g., Trenberth 1980; Angell 1986; Xu 1992). Others (e.g., Maruyama and Tsuneoka 1988) have suggested that if a relationship exists between SST variations (more explicitly, El Niño) and the stratospheric QBO, it is not an obvious one. Finally, it has been suggested (e.g., Gray 1992) that the stratospheric QBO might play a significant role in modulating the ENSO (El Niño–Southern Oscillation).

Corresponding author address: Dr. Marvin A. Geller, Institute for Terrestrial and Planetary Atmospheres, State University of New York at Stony Brook, Stony Brook, NY 11794-5000.
E-mail: MGELLER@ccmail.sunysb.edu.

In this paper, we present the results of some simple model calculations that assume time modulations of the equatorial wave momentum fluxes into the stratosphere. These time-varying wave momentum fluxes are used in a simple one-dimensional model of the QBO of the same type as that used by LH and HL. The model results suggest that even if the wave momentum fluxes into the stratosphere vary with time in a very simple fashion, the resulting QBO variations can be quite complex. To further illustrate the nature of the problem, we have performed calculations assuming that SST modulates the equatorial wave momentum fluxes into the stratosphere. Given the highly nonlinear nature of the problem, no simple relationship is seen between the SST-modulated input function to the model and the model output. These model results suggest that even if SST variations modulate the wave momentum fluxes into the stratosphere in a very simple fashion, the resulting QBO variations would not easily be identified as being associated with the SST variations.

2. Brief review of some QBO observations

Figure 1, an updated version of a figure in Naujokat (1986), shows that while the pattern of descending easterlies and westerlies that constitute the stratospheric QBO is very regular, there are large differences in the periods of individual QBO cycles. For instance, at 30 mb the period for transition from easterlies to westerlies is about 35 months during the easterly–westerly cycle of 1983–86, while during the 1972–73 cycle, this oscillation period is only about 21 months. Angell (1986) has examined this variability and compared it to three external factors, sea surface temperature, solar activity, and major volcanic eruptions. Figure 2 is an updated version of some results from Angell (1986). The QBO period at 30 hPa is seen to vary from less than 2 yr to about 3 yr, such that short periods tend to occur together over several cycles as do the oscillation cycles with longer periods. During this admittedly short period of record (1952–95), the QBO period appears to be varying in a quasiperiodic fashion where the period is about 10 yr. The other curve shows the SST variation in the eastern equatorial Pacific (0°–10°S, 180°–80°W). Angell made the following points. The variation in the QBO period looks to be completely unrelated to the SST curve. Although both the QBO period curve and the Wolf sunspot number curve showed decadal type changes, they did not appear to be closely related. The SST curve, on the other hand, showed more short period variability.

Trenberth (1980) and Xu (1992) have also examined SST variations, tropospheric variations, and the equatorial stratospheric QBO and reached the conclusion that the stratospheric QBO is statistically unrelated to SST and lower troposphere variations.

3. SSTs and equatorial atmospheric waves

Several mechanisms have been studied as sources for equatorial atmospheric waves. Mak (1969) suggested lateral forcing from subtropical latitudes to be an important factor. Hayashi and Golder (1978) considered models in which midlatitude forcing was imposed and then removed, and their results indicated that lateral boundary forcing did not provide the primary forcing of tropical waves in their experiments; however, there have been many studies that suggest that midlatitude circulations do have large impacts on tropical waves (e.g., Zangvil and Yanai 1980; Yanai and Lu 1983; Itoh and Ghil 1988). Other works have investigated variable tropical convection as a source for equatorial waves (e.g., Holton 1972; Salby and Garcia 1987). Hayashi (1970) and Lindzen (1974) suggested that wave–CISK (conditional instability of the second kind) might be an important mechanism for the forcing of atmospheric equatorial waves. The wave–CISK line of inquiry has been pursued by many investigators since then. Factors such as positive-only heating (e.g., Lau and Peng 1987), Ekman friction (e.g., Wang and Rui 1990), vertical wind shears (e.g., Lim et al. 1990; Zhang and Geller 1994), and phase shifts between the region of maximum low-level convergence and convection (Cho et al. 1994) have been considered. Recently, the entire concept of wave–CISK has been questioned. Emanuel et al. (1994) have suggested that convective heating, rather than providing an energy source for wave disturbances, actually acts to damp the waves. Emanuel et al. (1994) have suggested that a more reasonable theory for the origin of large-scale westerly propagating waves in the Tropics may be found in the WISHE (wave-induced surface heating) concept. In WISHE, the amount of evaporation (and convection) is controlled by the strength of the surface winds. There do seem to be some problems with both the wave–CISK and WISHE theories, however. Observations indicate that the maximum convective activity lags behind the region where there is maximum surface wind convergence, but wave–CISK theory suggests that they should be in phase. For eastward propagating disturbances in the easterlies, WISHE theory suggests that the regions with maximum convective activity should occur in advance of the maximum surface wind convergence. This being the case, one might conclude that the forcing mechanisms for equatorial atmospheric waves are not well understood at the present time.

We will be hypothesizing different scenarios for the nature of the variations of the easterly and westerly wave momentum fluxes into the stratosphere. Zhang and Geller (1994) have used a simplified linear model to study the stability of equatorial waves and its dependence on the vertical shear of the mean zonal flow. They found that the eastward propagating equatorial waves showed preferred growth when the vertical shear was easterly, that is to say, increasing easterlies with altitude, while

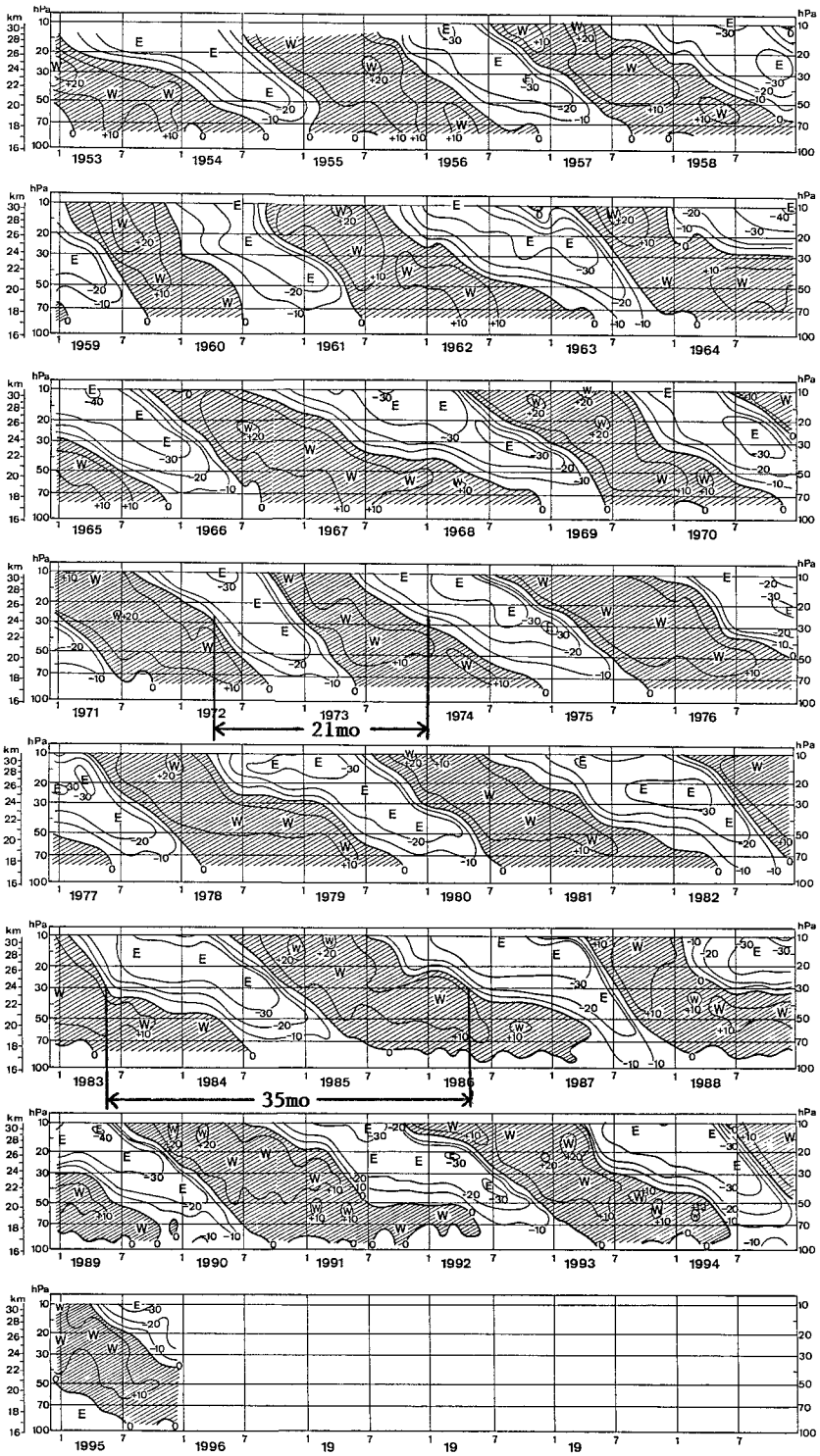

FIG. 1. Time–height section of monthly mean zonal winds (m s^{-1}) at equatorial stations Canton Island, 3°S, 172°W (January 1953–August 1967); Gan/Maledive Islands, 1°S, 73°E (September 1967–December 1975); and Singapore, 1°N, 104°E (since January 1976). Isopleths are at 10 m s^{-1} intervals. [Update from Naujokat (1986).] The periods of the complete easterly to westerly wind reversals at 30 hPa are indicated for the 1972–73 and 1983–86 cycles.

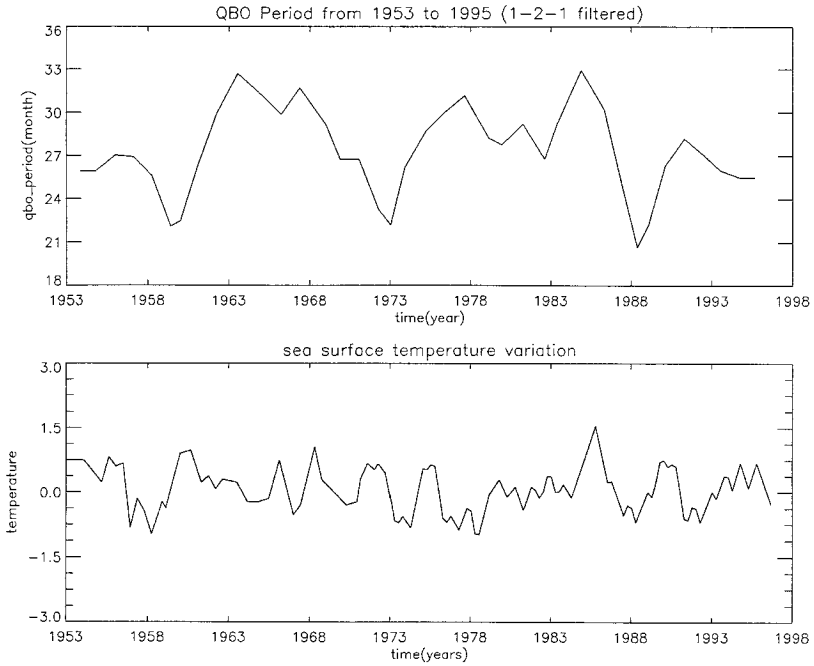

FIG. 2. Top: Time series of the period of the QBO at 30 hPa from the data shown in Fig. 1. A 1–2–1 filter has been applied in producing this curve. Bottom: Time series of the sea surface temperature in the eastern equatorial Pacific (0°–10°S, 180°–80°W). A double application of a 1–2–1 filter was used in producing this curve.

the westward propagating waves showed increased wave growth when the vertical shear was westerly. Also, when the shear conditions implied enhanced growth rates for waves propagating in one direction, there was suppression of wave growth rates for waves propagating in the other direction. If we assume that wave sources in the equatorial Pacific dominate the global situation (as appears feasible), then eastward propagating waves in the lower stratosphere might be enhanced under easterly shear conditions in that region relative to westward propagating waves, with the opposite situation being the case under westerly vertical shear conditions there. We expect easterly vertical shear conditions to preferentially exist in the equatorial Pacific under El Niño conditions with westerly shear conditions preferentially existing under La Niña conditions. With this hypothetical scenario in mind, we can simply relate the strength of easterly and westerly momentum fluxes into the lower stratosphere to SST variations in the equatorial Pacific, which are known to vary on many timescales, including biennial and longer periods (Rasmusson et al. 1990). Given this scenario, we expect easterly momentum fluxes to maximize when westerly momentum fluxes are at a minimum; that is, there is a 180° phase difference between the magnitudes of the easterly and westerly momentum fluxes for this wave–CISK model.

Another physical model is motivated by the picture of easterly and westerly momentum fluxes maximizing together, as would be the case if they were being forced by quasi-stationary time-varying convective regions. This is the physical picture that was considered by Holton (1972) and Salby and Garcia (1987). Since both the easterly and westerly momentum fluxes increase or decrease together in this model, there is a 0° phase difference between the magnitudes of the easterly and westerly momentum fluxes for this convective forcing model.

Assuming then that some factors are modulating the easterly and westerly momentum fluxes into the lower stratosphere, such as those mentioned in this section, we inquire as to how the equatorial circulation might respond.

4. QBO model

LH and HL used a one-dimensional model to illustrate how the westerly propagating equatorial Kelvin and the easterly propagating mixed Rossby–gravity wave interactions with the mean zonal flow give rise to a QBO. The results from these simple models agree in many respects with the observations. Several works followed that further elucidated the workings of the QBO. These included a two-dimensional model by Plumb and Bell (1982) and later attempts to model this phenomenon in three dimensions (e.g., Takahashi and Boville 1992).

We use here the same one-dimensional modeling approach used by LH and HL, the one difference being the inclusion of time-dependent forcing. Briefly, the LH and HL models take specified westerly and easterly momentum fluxes at the lower boundary (taken to be the

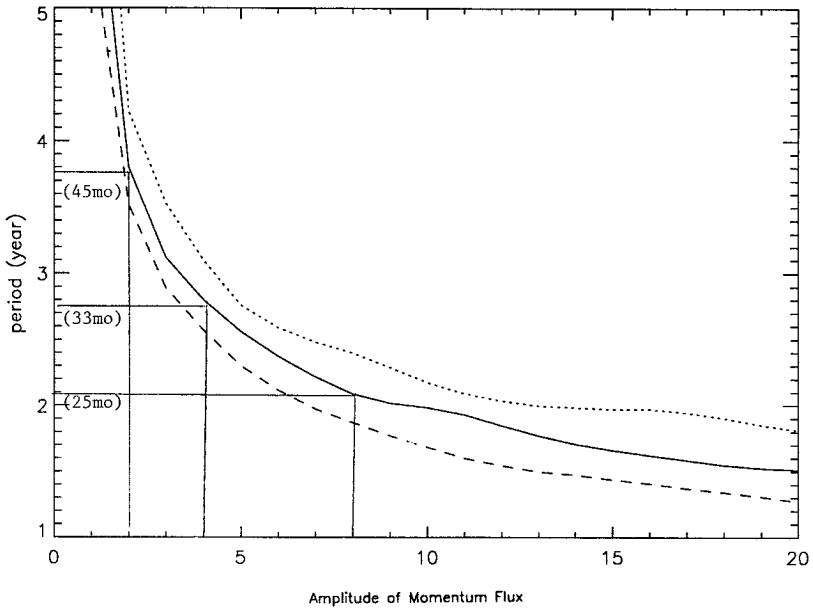

FIG. 3. Curves showing the calculated dependence of modeled QBO period (in yr) as functions of the vertical momentum fluxes (in units of 10^{-3} m^2 s^{-2}) from equatorial Kelvin and mixed Rossby–gravity waves. The solid curve is for a vertical diffusion of 3×10^3 cm^2 s^{-1}. The dashed (dotted) curve is for a vertical diffusion of 4.5×10^3 cm^2 s^{-1} (1.8×10^3 cm^2 s^{-1}).

tropopause). The absorption of these waves is parameterized by calculating the waves' group velocities and dissipating the waves according to the time that the waves' energy flux is exposed to the damping effect of Newtonian cooling (as in HL). The momentum flux convergence or divergence implied by this wave dissipation is calculated, and this momentum flux convergence or divergence is used in the zonal equation of motion to determine the time evolution of the mean zonal flow. Plumb (1982) has elegantly illustrated how these processes, plus diffusion, lead to a QBO having many of the characteristics of the observations.

Our calculations are done with the same choice of parameters as in HL. The Kelvin wave has zonal wavenumber 1, and the mixed Rossby–gravity wave has zonal wavenumber 4. The Newtonian cooling coefficient increases with altitude to a value of (7 days)$^{-1}$ at 30 km and above. The phase speed of the Kelvin wave is $+30$ m s^{-1}, while the phase speed of the mixed Rossby–gravity wave is -30 m s^{-1}. The diffusion coefficient is taken to be 3×10^3 cm^2 s^{-1}. A semiannual forcing is taken to exist above 28 km, as was done in the original work of LH and HL, although this has been shown to be unnecessary by Plumb (1977).

Plumb (1977) has derived a relationship for this problem that gives the period of the derived oscillation. This relationship clearly shows that the oscillation period decreases with increasing wave momentum fluxes at the lower boundary, with all other factors held constant. This is easily understood since the greater the momentum flux, the faster the descent velocity of the shear zones must be, and hence the shorter the oscillation period. The curve we have calculated for the dependence of the QBO period as a function of the Kelvin and mixed Rossby–gravity wave momentum fluxes at the lower boundary is shown in Fig. 3. One clearly sees the monotonic decrease of the oscillation period with increasing wave amplitudes. The two other curves shown in this figure are results for the dissipation coefficient scaled by 1.5 and 0.6. This does alter the period of the oscillation but not nearly so markedly as do variations in the wave amplitudes. In Fig. 3, there are three indicated values of the wave momentum fluxes at the model lower boundary, which is 100 mb. These are 2, 4, and 8 ($\times 10^{-3}$ m^2 s^{-2}), which correspond to oscillation periods 45 months, 33 months, and 25 months, respectively. These values of the momentum forcing will be used often in the paper's calculations that are shown in the next section.

5. Response to time-varying forcing

The time-varying forcing used for our first calculations with periodically varying momentum forcing is shown schematically in Fig. 4. The momentum forcing is composed of a steady forcing with equal easterly and westerly momentum fluxes plus a time-varying flux in which the westerly and easterly momentum fluxes are modulated sinusoidally with an amplitude equal to the steady fluxes. Thus, both the westerly and easterly momentum fluxes vary sinusoidally from twice their steady value to zero. This is the case in which the magnitudes

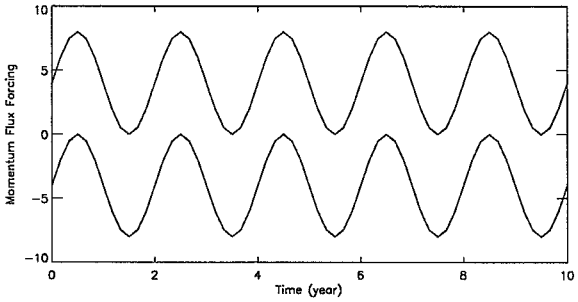

FIG. 4. Schematic illustration of steady wave forcing with momentum fluxes of $\pm 4 \times 10^{-3}$ m^2 s^{-2} and periodic forcing where the total forcing is given by the steady forcing, but with $4 \times 10^{-3} \sin[2\pi \times t(2 \text{ yr})^{-1}]$ m^2 s^{-2} added to both the westerly and easterly forcings.

of the easterly and westerly momentum flux magnitudes vary in phase by 180°. This corresponds to the Zhang and Geller (1994) predictions for wave–CISK. Figure 5 shows the resulting wind oscillations with steady easterly and westerly forcings of magnitude 2, 4, and 8×10^{-3} m^2 s^{-2} with time-varying momentum forcings of the same magnitude being added, as was illustrated in Fig. 4. The period of the time-varying forcing is taken to be 2 yr. Note that although the time-averaged forcings in these three cases would imply QBO periods of 45, 33, and 25 months (see Fig. 3), the resulting periods in all the three cases shown in Fig. 5 are approximately 2 yr, which is the period of the sinusoidally varying forcing. *Thus, the addition of the sinusoidally varying forcing serves to phase lock the resulting period to the period at which the momentum forcing is modulated.*

Of course, the previous case in which the time-varying forcing has the same magnitude as the steady forcing is very extreme. Figure 6 shows the results of a calculation where the steady momentum forcing at the lower boundary is 4×10^{-3} m^2 s^{-2} and the time varying forcing has magnitude 0 in case (a) and has magnitude 2×10^{-3} m^2 s^{-2} in cases (b)–(f). The period of the time-varying forcing is 1 yr in case (b), 2 yr in case (c), 3 yr in case (d), 4 yr in case (e), and 8 yr in case (f). Note that, as indicated in Figs. 3 and 6a, the resulting QBO period for a steady forcing of 4×10^{-3} m^2 s^{-2} is about 33 months. The resulting periods are about 3 yr for case (b), about 2 yr for case (c), 3 yr for case (d), and 4 yr for case (e). The result in case (f) is complicated with an initial tendency toward a very long period at low altitudes and a shorter period at higher altitudes but which gives an oscillation of period about 33 months at midstratospheric levels. *Figure 6 shows that there is a tendency for phase locking to occur when the time-varying forcing has sufficiently large amplitude (one-half of the steady forcing in this case), when the period of the time-varying forcing is near the period that results from the steady forcing alone, and when variation of the magnitudes of the easterly and westerly momentum fluxes has a 180° phase difference.* When the period of the time-varying forcing is either very much longer or shorter

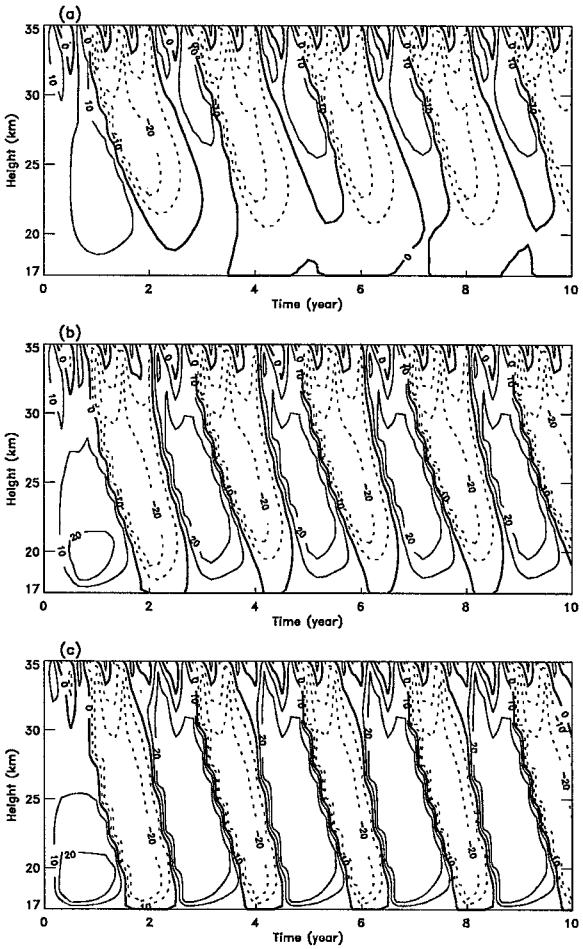

FIG. 5. Calculated mean zonal flow variations with steady plus 2-yr periodic forcing for the Kelvin and Rossby–gravity waves. The amplitude of the periodic component is the same as the steady component; (a) $\overline{u'w'} = \pm 2 \times 10^{-3}$ m^2 s^{-2}, (b) $\overline{u'w'} = \pm 4 \times 10^{-3}$ m^2 s^{-2}, and (c) $\overline{u'w'} = \pm 8 \times 10^{-3}$ m^2 s^{-2}. Solid lines indicate westerlies, and dashed lines indicate easterlies. Units are m s^{-1}.

than the period resulting from the steady forcing alone [cases (b) and (f)], there appears to be some sort of a ''beating'' between the period of the time-varying forcing and the oscillation resulting from the steady forcing.

Figure 7 shows some cases in which the magnitude of the time-varying forcing is one-quarter of the steady forcing. The steady momentum forcing at the lower boundary is 8×10^{-3} m^2 s^{-2} in cases (a)–(d), and the time varying forcing has magnitude 2×10^{-3} m^2 s^{-2}. The period of this time-varying forcing is 1 yr in case (a), 2 yr in case (b), 3 yr in case (c), and 4 yr in case (d). The resulting period in all of these cases is consistent with that calculated in Fig. 3. It is about 25 months. There certainly is no phase locking taking place, but if one looks closely, one does see an indication of a lengthening of the resulting oscillation as the period of the time-varying forcing increases. This is most easily seen by looking at the wind oscillation after 4 years (when there is very little sensitivity to the initial conditions).

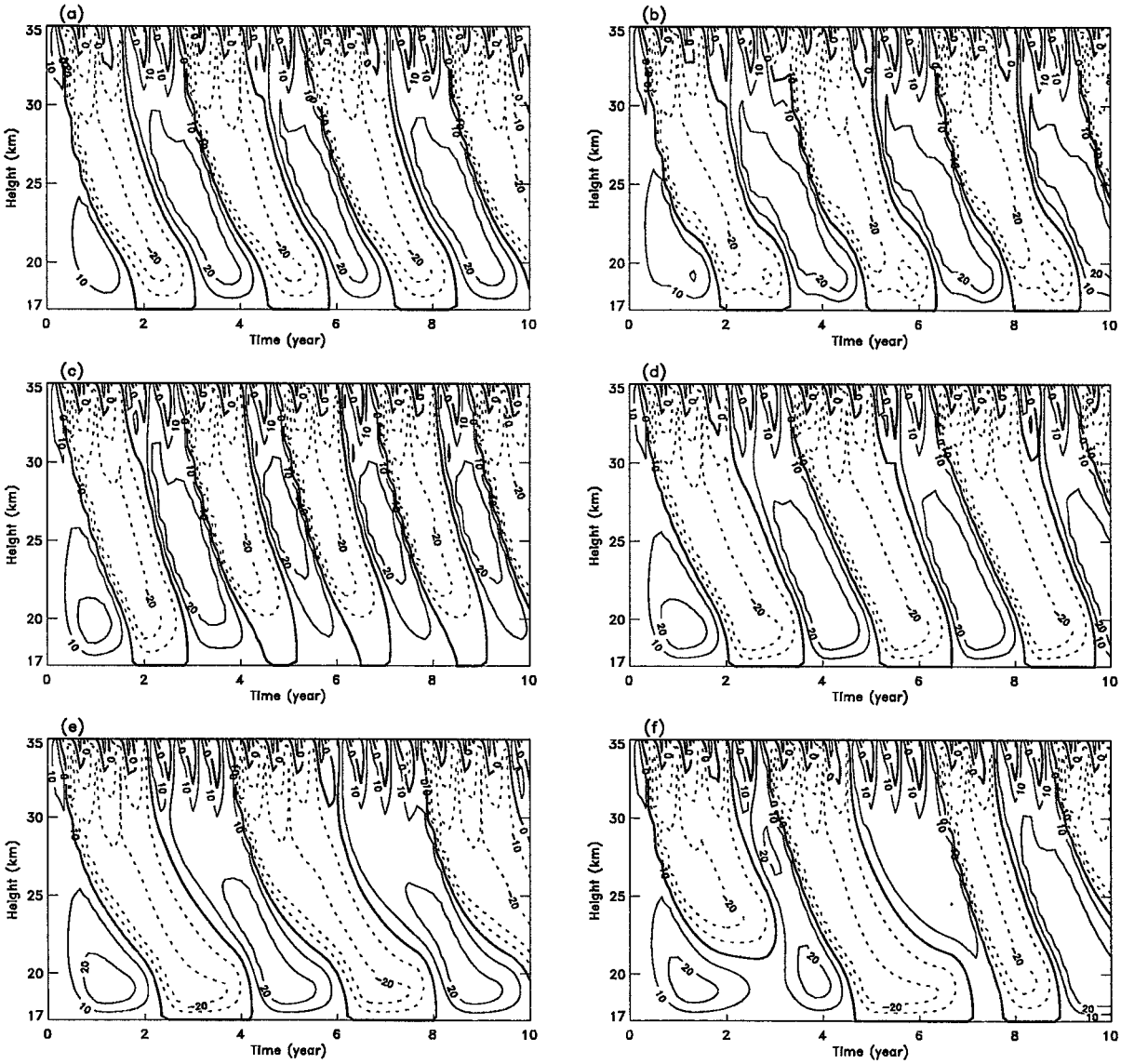

FIG. 6. (a) Calculated mean flow with Kelvin and Rossby–gravity wave forcings of $\pm 4 \times 10^{-3}$ m^2 s^{-2}. The other cases have the same steady wave forcings but with a periodic forcing of 2×10^{-3} m^2 s^{-2} sin[$(2\pi\, t$(n yr)$^{-1}$] added to both the Kelvin and Rossby–gravity wave forcings. For (b), n = 1. For (c), n = 2. For (d), n = 3. For (e), n = 4, and for (f), n = 8.

Note that the period of the two oscillations, starting after year 4, lengthens from (a) to (d). For reference, the horizontal line through these figures has length 4 years. *Thus, even when the amplitude of the time-varying momentum forcing is only one-quarter of the magnitude of the steady forcing, the period of the resulting oscillation is affected when the period of the time-varying forcing is close to that produced by the steady forcing alone in the case when the variations of the magnitudes of the easterly and westerly momentum fluxes are out of phase.*

We have performed many such calculations in which the Kelvin and mixed Rossby–gravity wave lower boundary momentum fluxes are given by constants of equal magnitude and opposite sign plus sinusoidally varying terms (as indicated schematically in Fig. 4). Figure 8 shows a summary of these results. In Fig. 8, the Kelvin wave forcing is given by $A_1 + A_2\sin(2\pi t/P) \times 10^{-3}$ m^2 s^{-2}, where $A_1 = 6$ (top), 4 (middle), and 2 (bottom), while the mixed Rossby–gravity wave forcing is given by $-A_1 + A_2\sin(2\pi t/P) \times 10^{-3}$ m^2 s^{-2}. The abscissa is A_2/A_1, and the ordinate is P (the period of the wave forcing modulation in years). For a given A_2/A_1, the period of the zonal wind oscillation is calculated for various forcing periods, P. Inside the shaded region, the period of the resulting ''QBO'' differs from that of the forcing by less than 0.1 months and inside the dashed curve, the period of the resulting QBO differs from that of the forcing by less than 1 month. Note the tongue

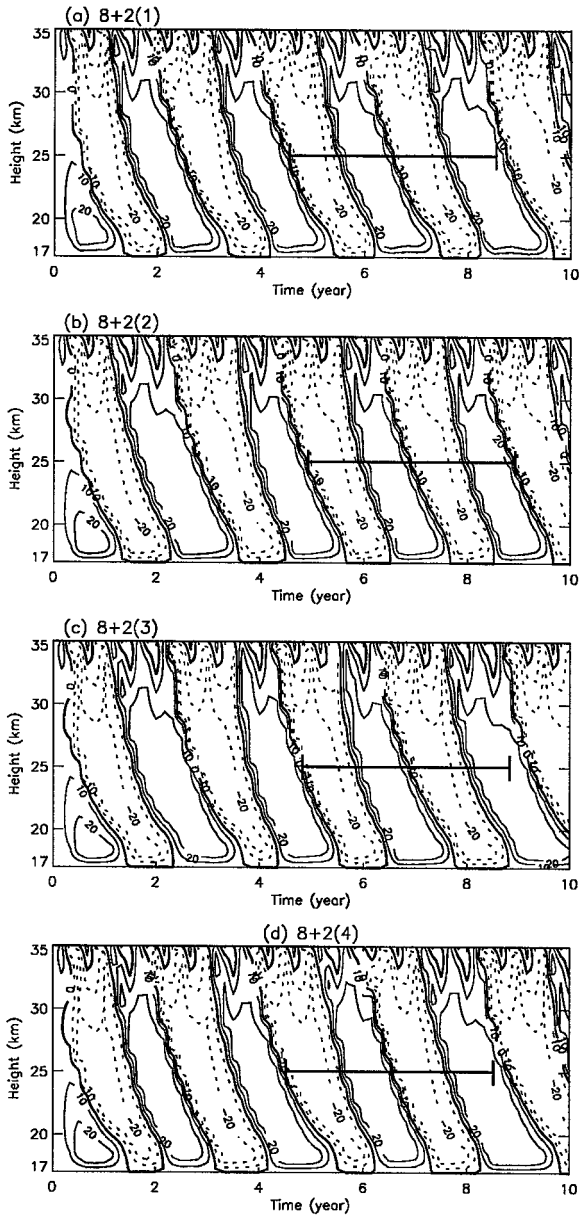

FIG. 7. Same as Fig. 6 except the steady wave forcing has magnitude 8 $m^2\ s^{-2}$ and n = 1 for (a), n = 2 for (b), n = 3 for (c), and n = 4 for (d). A horizontal bar, of length 4 yr, is put on the figure beginning at the onset of easterlies at 25 km at about year 5 of the simulation.

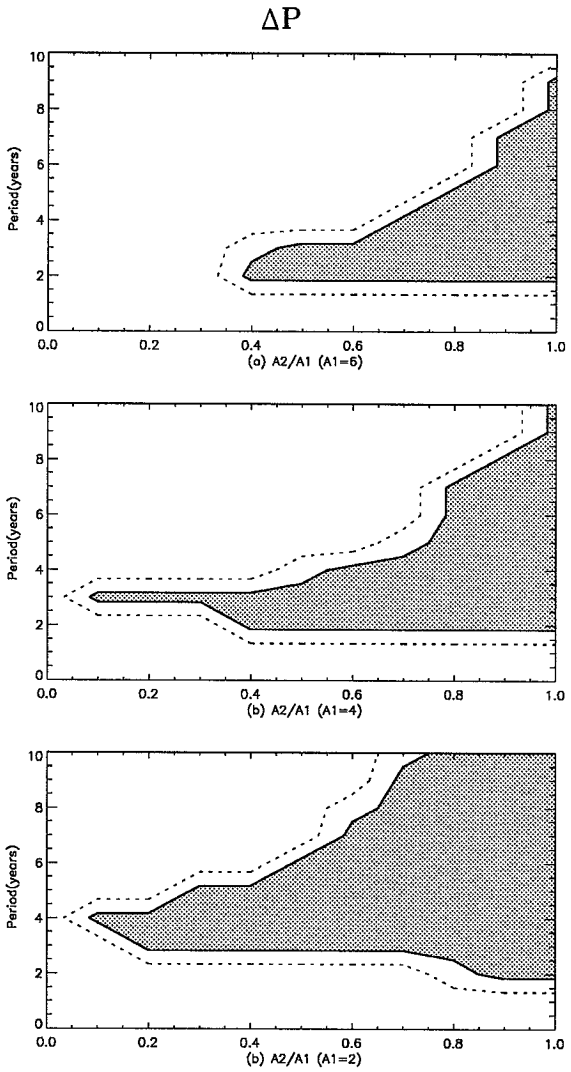

FIG. 8. Regime diagrams for steady plus periodic wave forcing of the mean flow. The magnitudes of the steady wave forcings are denoted by A_1 and the magnitude of the periodic wave forcings are denoted by A_2. The abscissa is $X = A_2/A_1$ and the ordinate is the period of the periodic forcings, P. Inside the dashed curve, the resulting wind oscillation's period differs from the forcing period by less than 1 month and inside the shaded region they differ by less than 0.1 months. The top panel shows results for $A_1 = 6 \times 10^{-3}$ m^2 s^{-2}. The middle curve shows results for $A_1 = 4 \times 10^{-3}$ m^2 s^{-2}, and the bottom panel shows results for $A_1 = 2 \times 10^{-3}$ m^2 s^{-2}. These results are for the easterly Kelvin wave forcing variations being 180° out of phase from the westerly mixed Rossby–gravity wave forcing.

shape of the computed curves. Referring to Fig. 3, one sees that a steady forcing of 6×10^{-3} m^2 s^{-2} corresponds to a QBO period of about 28 months, while steady forcings of 4×10^{-3} m^2 s^{-2} and 2×10^{-3} m^2 s^{-2} correspond to QBO periods of about 33 and 45 months, respectively. Note that the shape of these tongues implies that, when the variable component of the forcing has a period very close to the QBO period deduced from the steady forcing alone, phase locking occurs for small values of A_2/A_1. As the period of the forcing increases above that produced by the steady forcing alone, A_2/A_1 must increase for phase locking to occur; that is, the magnitude of the sinusoidal forcing must approach the steady forcing. The same is true for periods shorter than the QBO period implied by steady wave forcings with magnitude A_1, except that A_2/A_1 must increase faster for these shorter periods than for the longer periods to have phase locking.

In summary, the numerical experiments in this section illustrate that the behavior of a QBO model with a steady equatorial wave forcing plus a periodic component of

wave forcing in which Kelvin and mixed Rossby–gravity waves are modulated in the opposite sense is complex, but the following characteristics are found.

1) When the amplitudes of the periodic wave forcing are of the same order as the amplitudes of the steady forcing, there is a strong tendency for the resulting wind oscillation to be phase-locked to the wave forcing period if the wave forcing period is near that of the oscillation that results from the steady forcing alone.
2) When the periodic wave forcing is near to the period of the oscillation produced by the steady wave forcing alone, a tendency for phase locking is seen even when the amplitude of the periodic wave forcing is much less than that of the steady forcing.

We have also performed similar computations for various values for the phase difference between the easterly and westerly momentum fluxes. Essentially, no evidence of phase locking is seen for the 0° case (in phase variation of the magnitudes of the easterly and westerly momentum fluxes), and for intermediate phase difference values between 0° and 180°, there is a greater tendency for phase locking near phase differences of 180° and less of a tendency toward phase differences of 0°.

6. Response to nonstationary, nonperiodic forcing

We have seen that the QBO-type responses to time-varying equatorial wave forcings can be quite complex, depending on the following factors: 1) the ratio of the amplitude of the time-varying wave forcing to the steady forcing, 2) the period of the wave forcing relative to the period produced by the steady wave forcing alone, and 3) the phase relationship between the time-varying Kelvin and mixed Rossby–gravity waves.

For these reasons, we expect that the period of the modeled QBO might be quite dissimilar to the curve characterizing the time dependence of the wave forcing. To explore this possibility, we have experimented with the QBO response to a wave forcing whose time dependence is that of the eastern equatorial Pacific SSTs shown in Fig. 2 in the two cases that correspond to a 180° phase difference between the variation of the magnitudes of the easterly and westerly momentum fluxes (corresponding to the wave–CISK case) and the variation for a 0° phase difference (corresponding to the convective forcing case).

The three panels of Fig. 9 show the calculated periods of the resulting equatorial wind oscillations when the Kelvin and mixed Rossby–gravity wave momentum forcings are generated as follows. For example, in the middle panel, a steady Kelvin wave momentum flux per unit mass of $+6 \times 10^{-3}$ m^2 s^{-2} is imposed at the lower boundary together with a steady mixed Rossby–gravity wave flux of -6×10^{-3} m^2 s^{-2}. The time-varying Kelvin wave flux is given by the normalized curve for the variation of SSTs in the eastern equatorial Pacific that is shown in Fig. 2, multiplied by 3×10^{-3} m^2 s^{-2}; a mixed Rossby–gravity wave flux is generated in a similar manner so that the magnitudes of the easterly and westerly momentum fluxes are varying out of phase. Note that these variations of the Kelvin and mixed Rossby–gravity wave fluxes are specified in the sense suggested by the theoretical modeling results for the CISK instability of these waves by Zhang and Geller (1994), the 180° phase difference case. The magnitudes of the steady-state and time-varying forcings are arbitrary except that in the middle panel, the chosen value for the steady forcing makes the averaged wind oscillation about 29 months, which is in reasonable agreement with observations (shown as the dashed curve in the middle panel). Note that the curve for the time variation of the SSTs (in Fig. 2) that provides the time modulation for the momentum forcing does not resemble at all the calculated curve for the time variation of the QBO period. It is interesting that the computed curve for the QBO period does very much look like the observations, however, in this case (correlation coefficient is 0.40). Although we have not shown the wind patterns produced by this model, they show good qualitative resemblance to the observations shown in Fig. 1.

Earlier, we have seen that the timescales of the time-varying forcing to which the QBO models respond most are those timescales near the QBO period produced by the steady forcing alone. Thus, we expect to see more rapid time variations in the QBO period when the steady forcing is larger than when it is smaller. This is indeed found to be the case, as is illustrated in the top and bottom panels of Fig. 9, which show the results for similar calculations to those shown in the middle panel, except the steady momentum forcings are 8 and 4 ($\times 10^{-3}$ m^2 s^{-2}) and the time-varying amplitudes are 4 and 2 ($\times 10^{-3}$ m^2 s^{-2}), respectively. Note that, as expected, the mean period is shorter for the larger steady momentum forcing and longer for the smaller steady forcing. Also, note that the curve for the QBO period is more rapidly varying in the top panel and smoother in the bottom panel, which is consistent with the QBO period curve responding to periods near that produced by the steady forcing alone.

Figure 10 shows the results of a calculation similar to that shown in the middle panel of Fig. 9; that is, a steady forcing of 6×10^{-3} m^2 s^{-2} and a time-varying forcing where the magnitudes of the Kelvin and mixed Rossby–gravity waves have the same value but opposite sign. This is the 0° case. Note that, in this case, the modeled QBO period shows little resemblance to observations (correlation coefficient is 0.08).

We have also computed the QBO period response for both the 0° and the 180° cases for a variety of initial conditions. In the 180° case, the curves for all of the different initial conditions soon converge (not shown here), whereas for the 0° case, the resulting curves for the QBO period show no such convergence (not shown here). This suggests that the phase-locking effect produced in the 180° case soon produces the same time

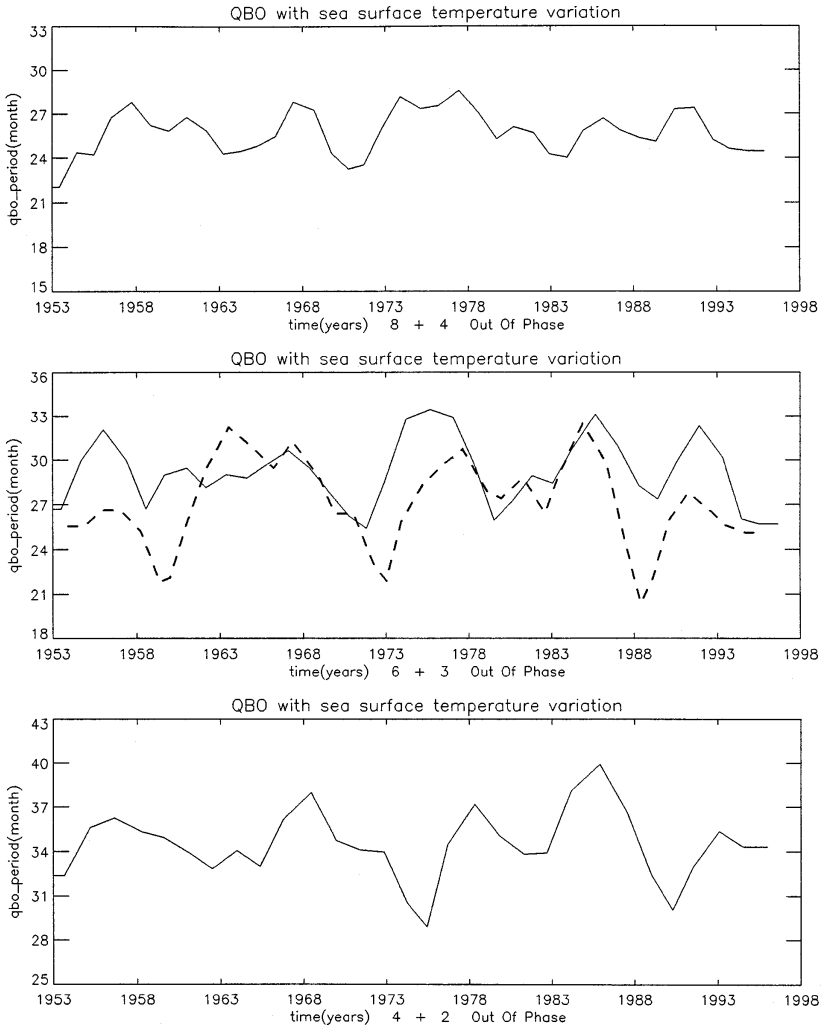

FIG. 9. The time variation of the calculated period of oscillation for the mean zonal wind. Top: The wave momentum forcing is given by the following. The Kelvin wave fluxes were generated by taking a steady wave forcing of magnitude 8×10^{-3} m^2 s^{-2} and a time-varying forcing of magnitude 4×10^{-3} m^2 s^{-2} multiplied by the normalized sea surface temperature plot shown in Fig. 2. The Rossby–gravity wave fluxes were generated by taking a steady wave forcing of -8×10^{-3} m^2 s^{-2} and the same periodic modulation as was used for the Kelvin waves. This is the 180° phase difference case. Middle: Same as top panel but with steady forcing magnitudes of 6×10^{-3} m^2 s^{-2} and time-varying forcing magnitudes of 3×10^{-3} m^2 s^{-2}. The dashed curve in this panel shows the observed curve from Fig. 2. Bottom: Same as previous panels but with steady forcing magnitudes of 4×10^{-3} m^2 s^{-2} and time-varying forcing magnitudes of 2×10^{-3} m^2 s^{-2}.

series for the smoothed QBO period, independent of initial conditions, but the 0° case gives results that depend critically on the initial conditions.

7. Summary and conclusions

LH and HL explain the existence of the QBO in terms of equatorial wave–mean flow interactions. That this is a nonlinear effect is obvious, especially when one considers that an oscillation results from a steady wave forcing. Here, we have considered the simple LH and HL one-dimensional model of the QBO with one effect added, the nonstationarity of the wave forcing. We have found that the solutions to this problem display a clearly nonlinear behavior. For a purely sinusoidal dependence of the wave forcing, phase locking exists between the period of the sinusoidal dependence and the resulting mean wind oscillation, depending on the amplitude of the sinusoidal forcing and its period of modulation. For phase locking to result, the period of the wave forcing must be relatively close to the period that results from the time-mean forcing alone, and the ratio of the time-varying component of the wave forcing to the steady wave forcing must be appreciable. The required period

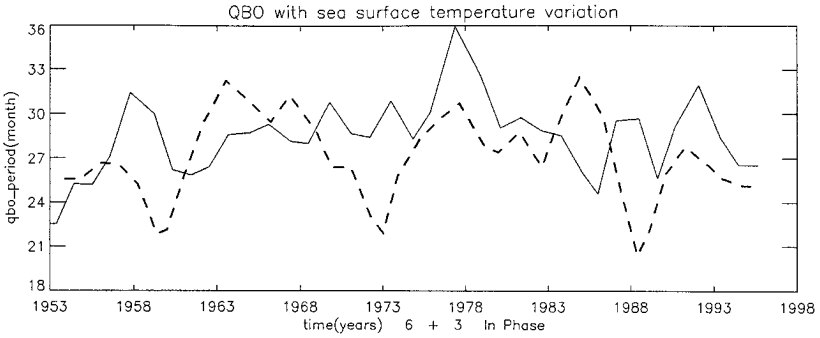

FIG. 10. Same as the middle panel of Fig. 9 but with the magnitudes of the easterly and westerly momentum fluxes varying in phase, i.e., the 0° case. Again, the observations from Fig. 2 are shown as the dashed curve.

of the wave forcing, relative to the period of the oscillation that results from the steady forcing alone, and the required amplitude of the time-varying forcing, relative to that for the time-averaged forcing, are shown to be interdependent in order for phase locking to occur.

If the time dependence of the prescribed wave forcing has a more complicated behavior, the time-varying wave period of the mean flow oscillation appears to be unrelated to the time-varying forcing, even though the wind oscillation behavior is mathematically a result of this time-varying wave forcing. This result shows the danger of using linear thinking to search for simple relationships between two parameters when their relationship is inherently nonlinear. Of course, this is an obvious statement. Yet such reasoning has been used in the literature to infer that there is no relationship between SST records and QBO behavior. A more reasonable procedure is to hypothesize a relationship between two variables that might be more linearly related. For instance, if one were attempting to prove the hypothesis that SST variations lead to variations in equatorial wave fluxes that, in turn, produce variations in the QBO period, one should search for a relationship between the wave fluxes themselves and the SSTs.

A particularly intriguing result is that when the prescribed equatorial wave momentum fluxes are taken to vary as the sea surface temperature in the eastern Pacific, the resulting modeled QBO period variation in time shows a striking resemblance to the observations. This does not demonstrate that these two are related as hypothesized, but it strongly suggests that year-to-year variations in the momentum fluxes forcing the QBO are related to SST variations and are rectified into longer time variations of the QBO period due to the effects discussed in this paper.[1] It furthermore suggests that these SST variations give rise to easterly and westerly momentum fluxes whose magnitudes vary somewhat out of phase by an amount closer to 180° than to 0°. Observational analyses are needed to examine these points.

Acknowledgments. This work was partly supported by the National Aeronautics and Space Administration's Earth Observing System project. The authors would like to thank Professor Duane E. Waliser for kindly supplying us with the SST variations from Comprehensive Ocean–Atmosphere Data Set data. We also thank Dr. Barbara Naujokat for providing us with the updated Fig. 1.

[1] It should be mentioned that there are also other physical mechanisms that might contribute to the irregularity of the QBO period. For instance, there is the weak coupling of the QBO with the annual cycle (e.g., Hamilton 1989).

REFERENCES

Angell, J. K., 1986: On the variations in period and amplitude of the quasi-biennial oscillation in the equatorial stratosphere, 1951–1985. *Mon. Wea. Rev.*, **114,** 2272–2278.

Cho, H.-R., K. Fraedrich, and J. T. Wang, 1994: Cloud clusters, Kelvin wave-CISK, and the Madden–Julian Oscillations in the equatorial troposphere. *J. Atmos. Sci.*, **51,** 68–76.

Emanuel, K. A., J. D. Neelin, and C. S. Bretherton, 1994: On large-scale circulations in convecting atmospheres. *Quart. J. Roy. Meteor. Soc.*, **120,** 1111–1143.

Gray, W. M., J. D. Shaeffer, and J. A. Knaff, 1992: Hypothesized mechanism for stratospheric QBO influence on ENSO variability. *Geophys. Res. Lett.*, **19,** 107–110.

Hamilton, K., 1989: Interhemispheric asymmetry and annual synchronization of the ozone quasi-biennial oscillation. *J. Atmos. Sci.*, **46,** 1019–1025.

Hayashi, Y., 1970: A theory of large-scale equatorial waves generated by condensation heat and accelerating the zonal wind. *J. Meteor. Soc. Japan*, **48,** 140–160.

——, and D. G. Golder, 1978: The generation of equatorial planetary waves: Control experiments with a GFDL general circulation model. *J. Atmos. Sci.*, **35,** 2068–2082.

Holton, J. R., 1972: Waves forced in the equatorial stratosphere generated by tropospheric heat sources. *J. Atmos. Sci.*, **29,** 368–375.

——, and R. S. Lindzen, 1972: An updated theory for the quasi-biennial oscillation of the tropical stratosphere. *J. Atmos. Sci.*, **29,** 1076–1080.

Itoh, H., and M. Ghil, 1988: The generation mechanism of mixed Rossby–gravity waves in the equatorial troposphere. *J. Atmos. Sci.*, **45,** 585–604.

Lau, K. M., and L. Peng, 1987: Origin of low-frequency (intraseasonal) oscillations in the tropical atmosphere. Part I: Basic theory. *J. Atmos. Sci.*, **44,** 950–972.

Lim, H., C.-P. Chang, and T.-K. Lim, 1990: Vertical wind shear effects

on Kelvin wave-CISK modes: Possible relevance to the 30–60 day oscillations. *Terr. Atmos. Oceanic Sci.,* **2,** 203–216.

Lindzen, R. S., 1974: Wave-CISK in the tropics. *J. Atmos. Sci.,* **31,** 156–179.

——, and J. R. Holton, 1968: A theory of the quasi-biennial oscillation. *J. Atmos. Sci.,* **25,** 1095–1107.

——, and C. Y. Tsay, 1975: Wave structure of the tropical stratosphere over the Marshall Islands area during 1 April–1 July 1958. *J. Atmos. Sci.,* **32,** 2008–2021.

Mak, M. K., 1969: Laterally driven stochastic motions in the tropics. *J. Atmos. Sci.,* **26,** 41–64.

Maruyama, T., and Y. Tsuneoka, 1988: Anomalously short duration of easterly wind phase of the QBO at 50 hPa in 1987 and its relationship to an El Niño event. *J. Meteor. Soc. Japan,* **66,** 629–633.

Naujokat, B., 1986: An update of the observed quasi-biennial oscillation of the stratospheric winds over the tropics. *J. Atmos. Sci.,* **43,** 1873–1877.

Plumb, R. A., 1977: The interaction of two internal waves with the mean flow: Implications for the theory of the quasi-biennial oscillation. *J. Atmos. Sci.,* **34,** 1847–1858.

——, 1982: The circulation of the middle atmosphere. *Aust. Meteor. Mag.,* **30,** 107–121.

——, and R. C. Bell, 1982: A study of the quasi-biennial oscillation on an equatorial beta-plane. *Quart. J. Roy. Meteor. Soc.,* **108,** 335–352.

Rasmusson, E. M., X. Wang, and C. F. Ropelewski, 1990: The biennial component of ENSO variability. *J. Mar. Sys.,* **1,** 71–96.

Reed, R. J., W. J. Campbell, L. A. Rasmussen, and D. G. Rogers, 1961: Evidence of the downward-propagating annual wind reversal in the equatorial stratosphere. *J. Geophys. Res.,* **66,** 813–818.

Salby, M. L., and R. R. Garcia, 1987: Transient response to localized episodic heating in the tropics. Part I: Excitation and short-time near-field behavior. *J. Atmos. Sci.,* **44,** 458–498.

Saravanan, R., 1990: A multiwave model of the quasi-biennial oscillation. *J. Atmos. Sci.,* **47,** 2465–2474.

Takahashi, M., and B. A. Boville, 1992: A three-dimensional simulation of the equatorial quasi-biennial oscillation. *J. Atmos. Sci.,* **49,** 1020–1035.

Trenberth, K. E., 1980: Atmospheric quasi-biennial oscillations. *Mon. Wea. Rev.,* **108,** 1370–1377.

Veryard, R. G., and R. A. Ebdon, 1961: Fluctuations in tropical stratospheric winds. *Meteor. Mag.,* **90,** 125–143.

Wang, B., and H. L. Rui, 1990: Dynamics of the coupled moist Kelvin–Rossby wave on an equatorial β plane. *J. Atmos. Sci.,* **47,** 397–413.

Xu, J.-S., 1992: On the relationship between the stratospheric quasi-biennial oscillation and the tropospheric Southern Oscillation. *J. Atmos. Sci.,* **49,** 725–734.

Yanai, M., and M. M. Lu, 1983: Equatorial trapped waves at the 200 mb level and their association with meridional convergence of wave energy flux. *J. Atmos. Sci.,* **40,** 2785–2803.

Yasunari, T., 1989: A possible link of the QBOs between the stratosphere, troposphere and sea surface temperature in the tropics. *J. Meteor. Soc. Japan,* **67,** 483–493.

Zangvil, A., and M. Yanai, 1980: Upper tropospheric waves in the tropics. Part I: Dynamical analysis in the wavenumber-frequency domain. *J. Atmos. Sci.,* **37,** 285–298.

Zhang, M., and M. A. Geller, 1994: Selective excitation of tropical waves in wave-CISK: The effect of vertical wind shear. *J. Atmos. Sci.,* **51,** 353–368.